Effects of electron correlation, electron-phonon coupling, and spin-orbit coupling on the isovalent Pd-substituted superconductor $SrPt_3P$

Kangkang Hu,[1,2] Bo Gao,[1] Qiucheng Ji,[1] Yonghui Ma,[1,3] Wei Li,[1,4,*] Xuguang Xu,[3] Hui Zhang,[4,5] Gang Mu,[1,4,†] Fuqiang Huang,[4,5] Chuanbing Cai,[2] Xiaoming Xie,[1,4] and Mianheng Jiang[1,3]

[1]*State Key Laboratory of Functional Materials for Informatics, Shanghai Institute of Microsystem and Information Technology, Chinese Academy of Sciences, Shanghai 200050, China*

[2]*Shanghai Key Laboratory of High Temperature Superconductors, Shanghai University, Shanghai 200444, China*

[3]*School of Physical Science and Technology, ShanghaiTech University, Shanghai 201210, China*

[4]*CAS Center for Excellence in Superconducting Electronics (CENSE), Shanghai 200050, China*

[5]*CAS Key Laboratory of Materials for Energy Conversion, Shanghai Institute of Ceramics, Chinese Academy of Sciences, Shanghai 200050, China*

(Received 10 January 2016; revised manuscript received 16 May 2016; published 17 June 2016)

We present a systematical study on the roles of interactions among electron correlation, electron-phonon coupling, and spin-orbit coupling in the isovalent Pd-substituted superconductor $SrPt_3P$. By using the solid state reaction method, the Pd element with the 4*d* orbital was successfully substituted in the strong spin-orbit coupling superconductors $Sr(Pt_{1-x}Pd_x)_3P$. As increasing the isovalent Pd concentrations without introducing any extra electron/hole carriers, the superconducting transition temperature T_c decreases monotonously. In addition, combining the data of resistivity and specific heat, as well as electronic band structure calculations, we found that the electron correlation is enhanced while the electron-phonon coupling and the spin-orbit coupling are suppressed by Pd substitution. Our results may provide significant insights in the natures of the interplay among the electron correlation, electron-phonon coupling, and spin-orbit coupling in superconductivity, and may also pave a route for understanding the mechanism of superconductivity in heavily 5*d*-based superconductors.

DOI: 10.1103/PhysRevB.93.214510

I. INTRODUCTION

The study of strong interplay among charge, spin, orbital, and lattice degrees of freedom in transition metal compounds has triggered enormous research interest in the communities of condensed matter physics and material physics. One of the most prominent example is the unconventional high-transition temperature (high-T_c) superconductivity induced by the strong electron correlation in the copper oxide and iron-based superconductors [1,2]. In those materials, apparently, the spin degree of freedom plays a vital rule, and the orbital degree of freedom is decoupled from that of spin. However, in strong spin-orbit coupling superconductors, such as the recently discovered platinum-based superconductors APt_3P (A = Ca, Sr, and La) [3–10], the systems display weak electron correlation effect. The relation among electron correlation, spin-orbit coupling, and even the electron-phonon coupling still remains unclear. To clarify the nature of the interplay among these interactions in superconductors is a crucial issue not only in condensed matter physics, but also in material science. Motivated by this issue, we focus our great attention on the isovalent Pd-substituted platinum-based superconductors $SrPt_3P$, where the strength of the electron correlation, electron-phonon coupling, and spin-orbit coupling can be tuned by the Pd concentration without introducing any extra electron or hole carriers into the system. This physics is quite different from the case that of the lanthanum-based superconductor $LaPt_3P$, where the extra electron is injected into the system as strontium of $SrPt_3P$ is replaced by lanthanum leading to the decrease of the total density of states (DOS) at the Fermi level, which results in the suppression of superconducting transition temperature T_c [7].

In this paper, the Pd element with strong electron correlation of the 4*d* orbital was successfully substituted to the site of Pt in strong spin-orbit coupling superconductor $SrPt_3P$. The crystal lattice is found to shrink along the *c* axis and expand along the *a* axis monotonously as increasing the Pd concentrations. Importantly, we find that the superconducting transition temperature T_c decreases with Pd substitution, which could not be attributed to the physics of changes of the DOS at the Fermi level, the impurity scattering and the pressure effect. Our investigations suggest that the interplay among the electron correlation, electron-phonon coupling, and spin-orbit coupling plays a vital role for the change of the superconducting behaviors.

II. EXPERIMENTS

The samples in this work are prepared via solid state reaction from the pure elements [11]. Firstly, we put stoichiometric amounts of platinum powder (purity 99.97%, Alfa Aesar), red phosphorus powder (purity 99.9%, Aladdin), and strontium pieces (purity 98%+, Alfa Aesar) together and ground them in a mortar. After that, the mixture is pressed into a small pellet and then sealed in a clean vacuum quartz tube. All the weighing and mixing procedures are carried out in a glove box with a protective argon atmosphere. The tube is heated up to 400 °C and held for 10 hours to prevent red phosphorus from volatilizing so quickly, and calcined at 900 °C for two days. The sintered pellet is reground and further annealed at 900 °C within an argon-filled quartz tubes for three days. The

*liwei@mail.sim.ac.cn
†mugang@mail.sim.ac.cn

doped samples $Sr(Pt_{1-x}Pd_x)_3P$ are prepared with adding a corresponding amount of palladium powder (purity 99.95%, Alfa Aesar) using the same method as mentioned above.

The structure of the obtained samples are checked using a DX-2700 type powder x-ray diffractometer. The magnetic susceptibility measurements are carried out on the magnetic property measurement system (Quantum Design, MPMS 3). The electrical resistance is measured using a four-probe technique on the physical property measurement system (Quantum Design, PPMS). We employ the thermal relaxation technique to perform the specific heat measurements on PPMS. The temperatures of the sample platform have been calibrated under different magnetic fields.

III. RESULTS AND DISCUSSIONS

A. Crystal structure

The crystal structure of this system has been reported by T. Takayama *et al.* previously [3], as shown in Fig. 1(a). Here we concentrate on the influences on the crystal lattice by the Pd substitution. For this reason, we measure the powder x-ray diffraction (XRD) on this series of materials, and the diffraction patterns are shown in Fig. 1(b). It is found that the main diffraction peaks can be indexed to the tetragonal structure with the space group $P4/nmm$. The black line represents the parent compound $SrPt_3P$. The asterisks refer to some unknown impurities which was also observed by T. Takayama *et al.* [3]. With the increase of the amount of Pd (x), there is no obvious increase of the impurity phases. However, the positions of diffraction peaks start to move apparently when x changes from 0 to 0.4, which points to the variation of the size of the crystal lattice. This tendency can be seen clearly in Fig. 1(c), where we enlarge the region near the (220) diffraction peak as an example.

To investigate the influences on the crystal lattice by the Pd substitution quantitatively, we obtain the lattice parameters by fitting the XRD data using the software Powder-X [12]. The results are shown in Fig. 1(d). As is shown in the graph, the crystal lattice shows a shrinkage along the c axis, while it expands along the a axis with the increase of doping. This tendency is very similar to that observed in $4d$- and $5d$-metal-doped iron arsenides $SrFe_{2-x}M_xAs_2$ (M = Rh, Ir, Pd) [13], which proves that Pd atoms take the place of Pt atoms leading to the alteration of cell parameters. In the high doping region above 0.4, the variation of the lattice parameters becomes gentle, indicating the limit of the chemical substitution. We note that this is a common phenomenon in some chemical doped materials, and such a saturated feature has been reported elsewhere [14]. Moreover, we noticed that the changes in the lattice parameters along the a and c axis almost compensate for each other, which leads the unit cell volume to show only a slight increase (about 0.3%) throughout the whole substituting range.

B. Superconducting transition temperature

In order to study the effect of Pd doping on the superconducting properties, we perform the temperature dependent magnetization and resistivity measurements on all the samples

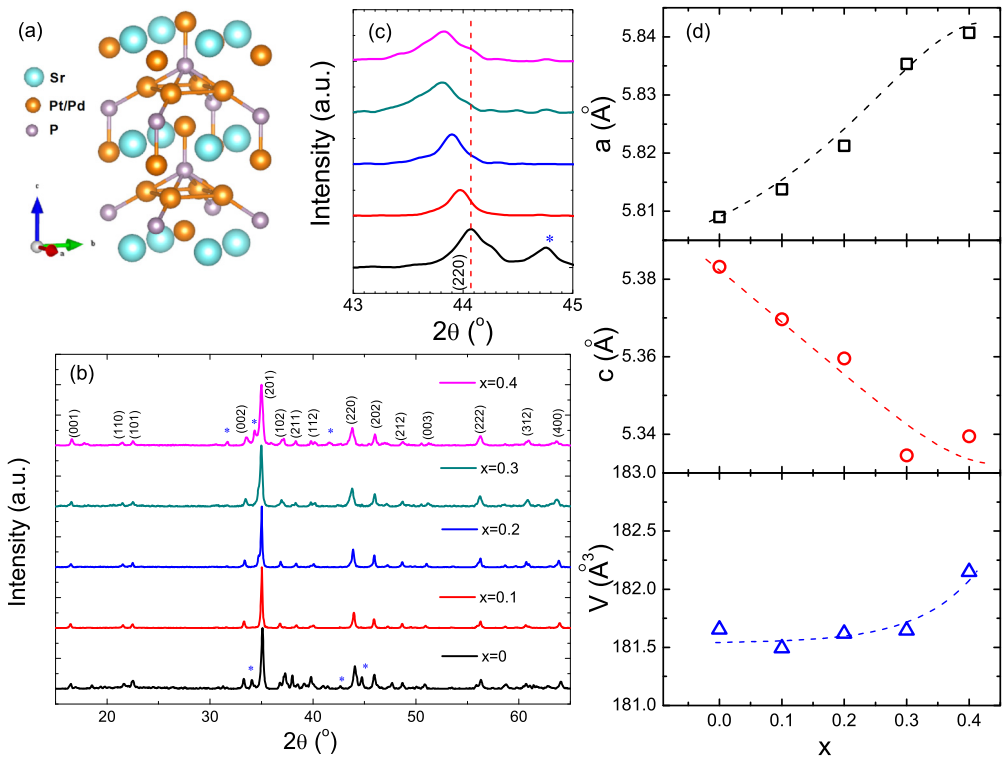

FIG. 1. (a) Crystal structure of $SrPt_3P$. Pd element is substituted into the site of Pt. (b) X-ray diffraction patterns for the $Sr(Pt_{1-x}Pd_x)_3P$ samples with $0 \leqslant x \leqslant 0.4$. (c) An enlarged view of the (220) peak. It is clear that the peak shifts monotonously to the left direction with doping. (d) Doping dependence of the lattice constants and unit cell volume.

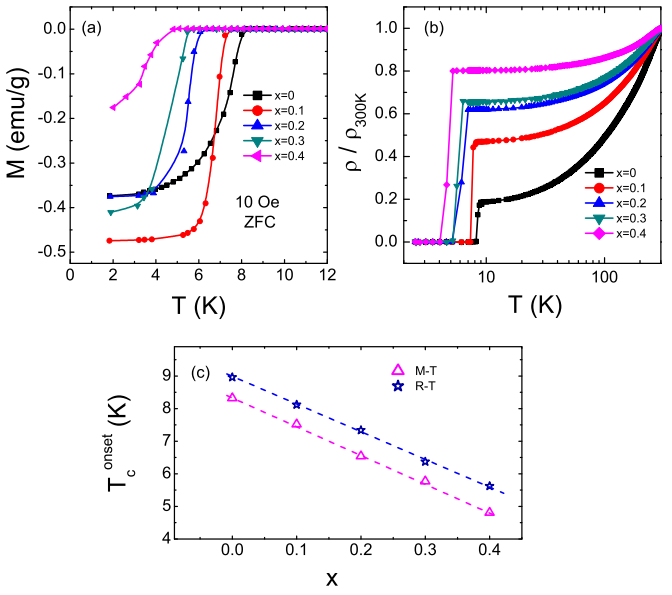

FIG. 2. (a) Temperature dependence of the dc magnetic susceptibility for $Sr(Pt_{1-x}Pd_x)_3P$ samples with $0 \leqslant x \leqslant 0.4$. The data were measured via the zero-field-cooling (ZFC) mode under the field of 10 Oe. (b) Temperature dependence of the normalized resistivity. (c) Doping dependence of the onset superconducting transition temperature. The blue and purple lines were defined by the $\rho - T$ and $M - T$ curves, respectively.

we synthesized. The temperature dependence of dc magnetic susceptibility is shown in Fig. 2(a), where we can see a sharp decline to the negative sides of the data for each sample with different doping. The clear diamagnetic signal indicates the occurrence of the superconducting transition and the onset transition point defines the critical transition temperature T_c. With the increase of amount of Pd, the value of T_c reduces apparently. This tendency is confirmed by the resistivity data, which is shown in Fig. 2(b). Clear superconducting transitions to zero resistance are observed on all the samples with different doping levels. The onset transition temperatures determined from this figure, along with that determined from the $M - T$ curves, are displayed in Fig. 2(c). The blue symbols are obtained from the magnetization measurements while the purple ones are defined by the resistivity measurements. It can be seen that the two sets of T_c values evolute parallelly and decrease linearly with x.

Generally speaking, the suppression of superconducting transition temperature T_c is usually related to the changes of DOS at Fermi level, as has been reported in the lanthanum replaced superconductor $LaPt_3P$ by comparing with $SrPt_3P$ [7]. However, the calculated DOS by means of density functional theory demonstrated that the DOS around the Fermi level remains almost the same for different concentrations of Pd dopants [see Fig. 5(d)], which will be discussed in the next section in detail. This result is reasonable since the palladium is isovalent to platinum making the carriers of the system remain unchanged. Thus, it rules out the possibility of the effect from the changes of DOS on superconductivity in our system. Another issue is the possible impurity scattering effect, which comes from the palladium substitution for platinum [15]. This possibility can also be ruled out since $SrPt_3P$ was reported to be an s-wave superconductor [3,10]. According to the Anderson's theorem [16], the nonmagnetic impurity does not lead to an apparent pair-breaking effect in a conventional s-wave superconductor, and thus does not suppress the transition temperature T_c apparently, which is in sharp contrast to that in a nodal superconductor, where the zero energy excitation spectra can be modified significantly by nonmagnetic impurities leading to the suppression of T_c [17]. In addition, we noticed that pressure can also effect the superconducting transition temperature T_c of this system [8]. By Pd substitution, we find that the unit cell volume increases very slightly, as shown in Fig. 1(d). Especially, this volume remains almost unchanged below $x = 0.3$, while T_c decreases clearly. Thus, we conjecture that such a volume change could not explain the nature of decrease of superconducting transition temperature T_c.

C. Electron correlation and electron-phonon coupling

Since the experimental observation of the suppression of the T_c does not originate from the changes of DOS at the Fermi level, the impurity scattering effect and the pressure effect, the T_c suppression is likely to be related to the interplay among the electron correlation, electron-phonon coupling, and the spin-orbit coupling. In order to clarify and distinguish the interplay among them, we first evaluate the strength of electron correlation from the coefficient of the quadratic term in the temperature dependence of resistivity, which is a measurement of the strength of electron-electron correlation [18,19]. The resistivity data in the low temperature above T_c for the two comparative samples with $x = 0$ and $x = 0.3$ were fitted using the formula $\rho = \rho_0 + AT^2$, where ρ_0 and A are the fitting parameters. As shown in Fig. 3, the fitting curves can roughly describe the experimental data in the low temperature, demonstrating the Fermi-liquid behavior. The coefficients of the quadratic term were determined to be $A = 3.1 \times 10^{-2}$ $\mu\Omega\,\mathrm{cm/K^2}$ and 4.5×10^{-2} $\mu\Omega\,\mathrm{cm/K^2}$ for the two samples, respectively, which suggests that the Pd substitution tends to enhance the electron correlation of

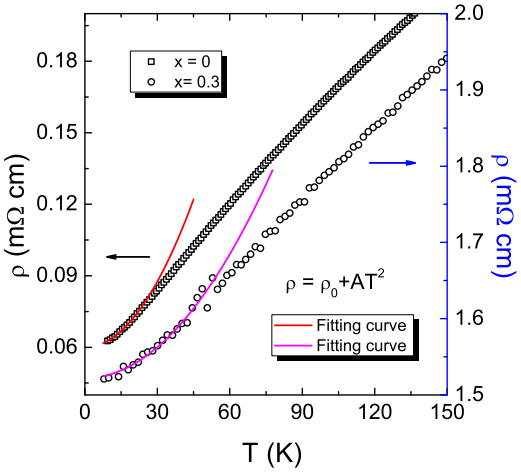

FIG. 3. Temperature dependence of resistivity at temperatures above T_c for two samples with $x = 0$ and $x = 0.3$. The solid lines show the fit in the low temperature range using the formula $\rho = \rho_0 + AT^2$.

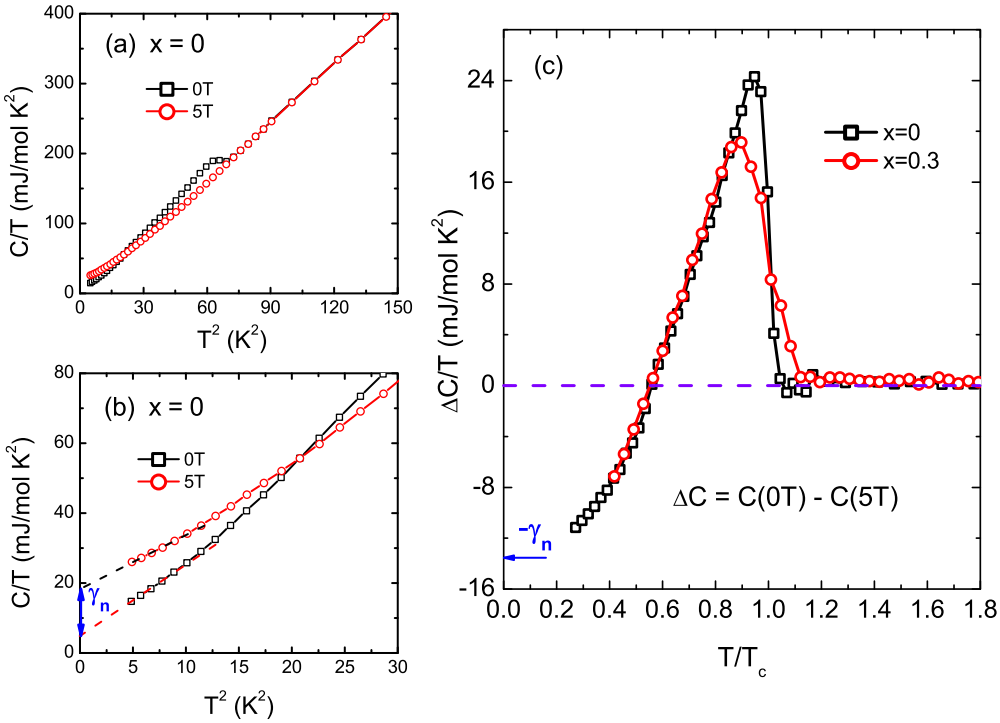

FIG. 4. (a) Raw data of specific heat for $x = 0$ plotted as C/T vs T^2. (b) Enlarged view of the same data in the low temperature region. The normal states electronic SH coefficient γ_n was obtained by linearly extrapolating the data at zero field and 5 T to 0 K (see the arrowed blue line). (c) Normalized temperature dependence of the electronic SH contribution (with the normal-state part subtracted) for two samples with $x = 0$ and $x = 0.3$. The arrow indicates the position of $-\gamma_n$.

this system. This tendency is expected as intuitively, since the bandwidth of Pd 4*d* orbitals is narrower than that of Pt 5*d* orbitals making the electron correlation in Pd 4*d* orbital electrons stronger than that in Pt 5*d* orbital electrons.

On the other hand, the electron-phonon coupling has been found to be responsible for superconductivity in the APt_3P (A = Ca, Sr and La) system [20]. In order to check this effect, we conduct the low-temperature specific heat (SH) measurements on two samples with $x = 0$ and $x = 0.3$ for comparison. As shown in Fig. 4(a), clearly the SH anomaly can be observed from the raw data under zero field, which is suppressed completely by a field of 5 T. The normal states electronic SH coefficient γ_n is obtained by linearly extrapolating the data at zero field and 5 T to 0 K, as indicated by the arrowed blue line in Fig. 4(b). The fitted value $\gamma_n = 13.54\,\mathrm{mJ/mol\,K^2}$ is comparable with the previous reports [3,8]. We note here that one mole means Avogadro number of unit cell with the chemical formula $[Sr(Pt_{1-x}Pd_x)_3P]_2$. The electronic SH in the superconducting states can be extracted by subtracting the data at 5 T from that at 0 T, $\Delta C = C(0T) - C(5\ \mathrm{T})$, since the SH data at 5 T reflect the situation of the normal states. As we have known, the SH in the normal states is composed contributions from the electrons and the phonons, which are not affected by the magnetic field [21,22]. Temperature dependence of $\Delta C/T$ of the two samples with $x = 0$ and $x = 0.3$ is shown in Fig. 4(c). The x coordinate has been normalized to T_c to facilitate the comparison. It is found that the data for the two samples coincide roughly with each other in a wide temperature range $0.4 \leqslant T/T_c \leqslant 0.9$. Such consistent behavior gives a strong implication that the two curves will evolve similarly to lower temperatures even to 0 K, leading to the almost same value of $-\gamma_n$ as denoted by the blue arrow. As for the SH jump induced by the superconducting transition, the sample with $x = 0.3$ displays a lower SH jump leading to a smaller value of $\Delta C/T|_{T_c}$, compared with the parent sample $SrPt_3P$. The amplitude of the ratio $\Delta C/\gamma_n T|_{T_c}$, which reflects the electron-phonon coupling strength, is 1.80 and 1.42 for the two samples with $x = 0$ and $x = 0.3$, respectively. Additionally, we should note that such a suppression of the electron-phonon coupling strength is similar to that reported in the Si-doped $SrPt_3P$ system [8].

D. Spin-orbit coupling and first-principles calculations

As we have known, the spin-orbit coupling strength is proportional to Z^4 (where Z is the atomic number; $Z_{Pt} = 78$ for Pt, and $Z_{Pd} = 46$ for Pd) [23]. The ratio $\Gamma = (\frac{Z_{Pt}}{Z_{Pd}})^4 = 8.3$ and consequently the spin-orbit coupling strength will be decreased dramatically when the platinum is substituted by palladium. In order to investigate the influence of Pd substitution on DOS and the spin-orbit coupling, accordingly clarify the origins for the suppression of T_c in superconductor $Sr(Pt_{1-x}Pd_x)_3P$ theoretically, we carried out the first-principles band structure calculations on the samples with $x = 0$, $x = 0.17$, and $x = 0.33$. The calculations were performed by using the pseudopotential-based code VASP [24] within the Perdew-Burke-Ernzerhof [25] generalized gradient approximation. Throughout the theoretical calculations, a 500 eV cutoff in the plane wave expansion and a $12 \times 12 \times 12$ Monkhorst $\vec{k}$ grid were chosen to ensure the calculation with an accuracy of

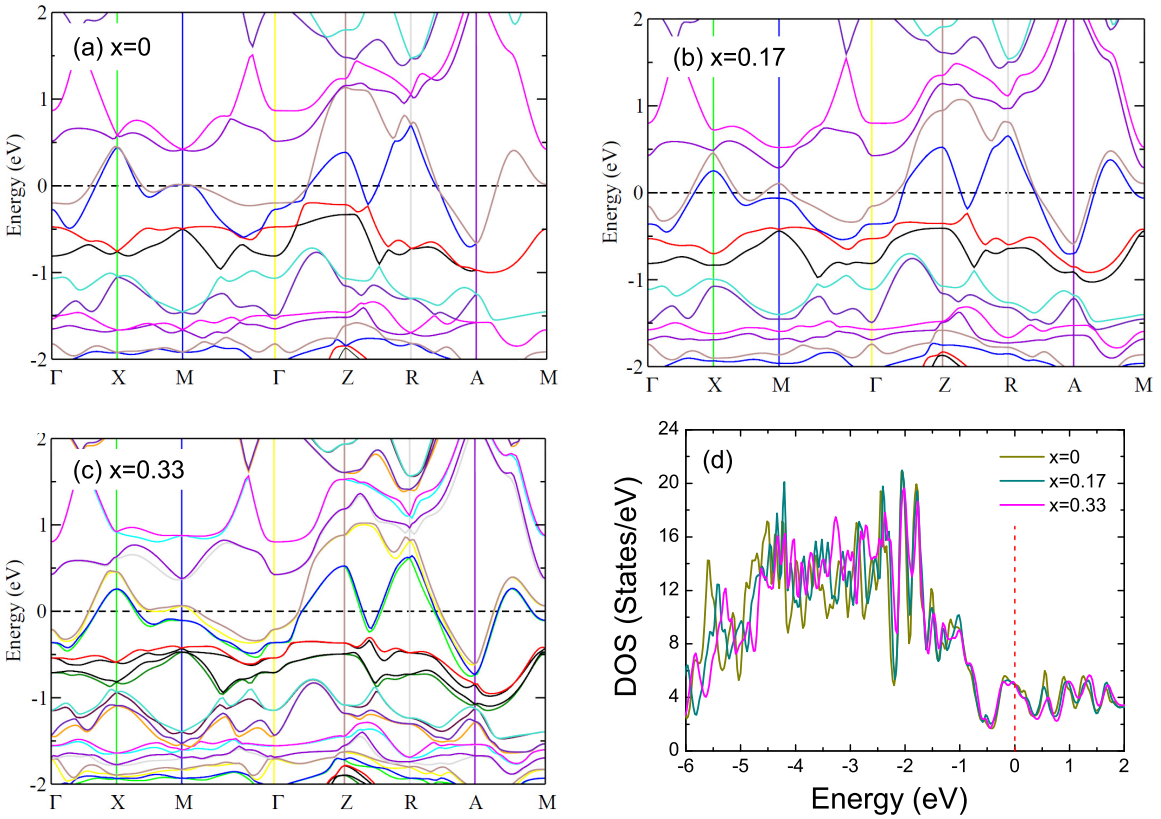

FIG. 5. The electronic band structure for $Sr(Pt_{1-x}Pd_x)_3P$ with doping (a) $x = 0$, (b) $x = 0.17$, and (c) $x = 0.33$. (d) The corresponding density of states (DOS) to the three samples. The Fermi energy was set to zero (dashed lines).

10^{-5} eV. The atomic coordinates were obtained by the relaxation based on the lattice parameters from experiments. Additionally, the spin-orbit coupling had been included throughout the calculations.

In Fig. 5, we show the energy band structures and their corresponding DOS. By comparing the energy band structures and DOS with different Pd contents, the low energy features of electronic structures remain almost the same, except for lifting the degenerate bands and changing their dispersion at some high symmetric momentum points around the Fermi level. This originates from the nature of 4*d* element Pd. When the atom Pt in $SrPt_3P$ is partially substituted by Pd, the high symmetry of the point group of the system was lowered leading to the lifting of some degenerate energy bands. Because the electron correlation is not involved in our calculations, the changes in the low energy dispersion due to the stronger electron-electron interaction in the Pd-substituted compounds could not be distinguished.

To quantitatively find the relation between electron correlation and spin-orbit coupling in the present isovalent Pd doped system, we further carried out the electron susceptibility calculations. The bare electron susceptibility $\chi_0(\vec{q})$ is given by:

$$\chi_0(\vec{q}) = \frac{1}{N_{\mathbf{k}}} \sum_{\mu\nu\mathbf{k}} \frac{|\langle \mathbf{k}+\vec{q},\mu|\mathbf{k},\nu\rangle|^2}{E_{\mu,\mathbf{k}+\vec{q}} - E_{\nu,\mathbf{k}} + i0^+} [f(E_{\nu,\mathbf{k}}) - f(E_{\mu,\mathbf{k}+\vec{q}})],$$

where $E_{\mu,\mathbf{k}}$ represents the band energy measured at Fermi level E_F, and $f(E_{\mu,\mathbf{k}})$ is the Fermi-Dirac distribution function for an eigenstate $|\mathbf{k},\mu\rangle$. In addition, $N_{\mathbf{k}}$ denotes the number of **k** points used for the irreducible Brillouin zone integration. The calculated real part of electron susceptibility is shown in Fig. 6, which demonstrates that the peak of electron susceptibility is suppressed as the Pd concentrations increase. This result suggests that the electron susceptibility of the system originating from the itinerant electrons with strong spin-orbit coupling is weakened by Pd substitution.

A previous study has shown that the inclusion of spin-orbit coupling in the calculations is responsible for a 23% increase in the strength of the electron-phonon coupling [9]. We argue that, in the present Pd-substituted $SrPt_3P$ system, the weakened spin-orbit coupling may be responsible for the suppression of

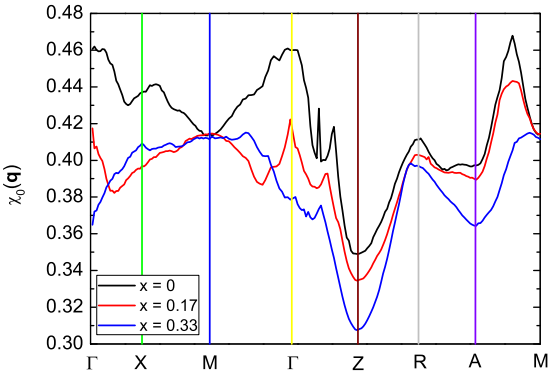

FIG. 6. The real part of bare electron susceptibility $\chi_0(\vec{q})$ along the path between high symmetric momentum points.

the electron-phonon coupling, which leads to the decrease of T_c. Our results also indicate that the electron correlation is not favorable to superconductivity.

IV. CONCLUSION

In conclusion, we have successfully substituted Pd elements into the position of Pt in the strong spin-orbit coupling superconductor $SrPt_3P$ and found that the doping of Pd not only leads to the change of lattice parameters but also suppresses the superconducting transition temperature T_c. Combining the experimental measurements and band structure calculations, it is concluded that, by influencing the electron-phonon coupling, the completing between the spin-orbit coupling and electron correlation may play a vital role in superconductivity of the present $5d$ electron system.

ACKNOWLEDGMENTS

We are thankful for the discussions with Prof. Diego A. Zocco and Prof. T. Hu. This work is supported by the Natural Science Foundation of China (No. 11204338, 11227902, and 11404359), the "Strategic Priority Research Program (B)" of the Chinese Academy of Sciences (No. XDB04040300), and the Youth Innovation Promotion Association of the Chinese Academy of Sciences (No. 2015187). This work is partly sponsored by the Science and Technology Commission of Shanghai Municipality (No. 14DZ2260700 and 14521102800).

[1] J. G. Bednorz and K. A. Müller, Z. Phys. B **64**, 189 (1986).
[2] Y. Kamihara, T. Watanabe, M. Hirano, and H. Hosono, J. Am. Chem. Soc. **130**, 3296 (2008).
[3] T. Takayama, K. Kuwano, D. Hirai, Y. Katsura, A. Yamamoto, and H. Takagi, Phys. Rev. Lett. **108**, 237001 (2012).
[4] C.-J. Kang, K.-H. Ahn, K.-W. Lee, and B. I. Min, J. Phys. Soc. Jpn. **82**, 053703 (2013).
[5] H. Chen, X. Xu, C. Cao, and J. Dai, Phys. Rev. B **86**, 125116 (2012).
[6] R. Szczęśniak, A. P. Durajski and Ł. Herok, Phys. Scr. **89**, 125701 (2014).
[7] I. A. Nekrasov and M. V. Sadovskii, JETP Lett. **96**, 227 (2012).
[8] B. I. Jawdat, B. Lv, X. Zhu, Y. Xue, and C.-W. Chu, Phys. Rev. B **91**, 094514 (2015).
[9] D. A. Zocco, S. Krannich, R. Heid, K.-P. Bohnen, T. Wolf, T. Forrest, A. Bosak, and F. Weber, Phys. Rev. B **92**, 220504(R) (2015).
[10] T. Shiroka, M. Pikulski, N. D. Zhigadlo, B. Batlogg, J. Mesot, and H.-R. Ott, Phys. Rev. B **91**, 245143 (2015).
[11] G. Mu, Y. Wang, L. Shan, and H. H. Wen, Phys. Rev. B **76**, 064527 (2007).
[12] C. Dong, J. Appl. Crystallogr. **32**, 838 (1999).
[13] F. Han, X. Zhu, P. Cheng, G. Mu, Y. Jia, L. Fang, Y. Wang, H. Luo, B. Zeng, B. Shen, L. Shan, C. Ren, and H. H. Wen, Phys. Rev. B **80**, 024506 (2009).
[14] Q. C. Ji, Y. H. Ma, K. K. Hu, B. Gao, G. Mu, W. Li, T. Hu, G. H. Zhang, Q. B. Zhao, H. Zhang, F. Q. Huang, and X. M. Xie, Inorg. Chem. **53**, 13089 (2014).
[15] K. K. Hu, B. Gao, Q. C. Ji, Y. H. Ma, H. Zhang, G. Mu, F. Q. Huang, C. B. Cai, and X. M. Xie, Front. Phys. **11**, 117403 (2016).
[16] P. W. Anderson, J. Phys. Chem. Solids **11**, 26 (1959).
[17] G. Xiao, M. Z. Cieplak, J. Q. Xiao, and C. L. Chien, Phys. Rev. B **42**, 8752 (1990).
[18] J. Paglione, M. A. Tanatar, D. G. Hawthorn, E. Boaknin, R. W. Hill, F. Ronning, M. Sutherland, L. Taillefer, C. Petrovic, and P. C. Canfield, Phys. Rev. Lett. **91**, 246405 (2003).
[19] F. Ronning, C. Capan, E. D. Bauer, J. D. Thompson, J. L. Sarrao, and R. Movshovich, Phys. Rev. B **73**, 064519 (2006).
[20] A. Subedi, L. Ortenzi, and L. Boeri, Phys. Rev. B **87**, 144504 (2013).
[21] G. Mu, B. Zeng, P. Cheng, Z. S. Wang, L. Fang, B. Shen, L. Shan, C. Ren, and H. H. Wen, Chin. Phys. Lett. **27**, 037402 (2010).
[22] G. Mu, J. Tang, Y. Tanabe, J. Xu, S. Heguri, and K. Tanigaki, Phys. Rev. B **84**, 054505 (2011).
[23] W. Li, X. Y. Wei, J. X. Zhu, C. S. Ting, and Y. Chen, Phys. Rev. B **89**, 035101 (2014).
[24] G. Kresse and J. Furthmuller, Phys. Rev. B **54**, 11169 (1996).
[25] J. P. Perdew, K. Burke, and M. Ernzerhof, Phys. Rev. Lett. **77**, 3865 (1996).